PEFFECT OF EXPOSURE TO SUPERCRITICAL WATER ON CORROSION BEHAVIOUR OF SELECTED MATERIALS

[1*] Monika ŠÍPOVÁ, [1] Daniela MARUŠÁKOVÁ, [1] Jan PROCHÁZKA

[1]CVŘ - Centrum výzkumu Řež, s.r.o., Husinec-Řež, Czech Republic, EU, [*] monika.sipova@cvrez.cz

https://doi.org/10.37904/metal.2022.4477

Abstract

Titanium stabilized stainless steel 08Ch18N10T is widely used in VVER nuclear power plants. The alloy 800H is a very promising structural material for application in future nuclear power plants working under more severe working conditions. Thus, both materials were exposed above the critical point of water at 395 °C, 25 MPa for 500 and 2700h. The effect of such exposures was evaluated based on analyses of microstructure via scanning electron microstructure involving chemical and crystallographic analyses. The thin oxide layers were further described by X-ray diffraction. The stainless steel 08Ch18N10T proved very good and comparable corrosion resistance with highly alloyed 800H at the given environment. In both cases, the oxide layer was very thin even after long exposure.

Keywords: Stainless steels, alloy 800H, supercritical water, corrosion

INTRODUCTION

The demand for energy is still increasing and thus the way to satisfy it is searched. The use of supercritical water in the nuclear field is thus the natural development of the widely used light water-cooled nuclear reactor. Supercritical water (SCW) exists above critical point of water (374 °C, 22 MPa) and it possesses properties [1], different from classic water, which can be effectively used in the production of energy. One of the possible ways can be the IV. generation of nuclear reactors. Among the six most perspective concepts is the supercritical water-cooled reactor (SCWR) [2]. In addition, the concept small modular reactor cooled by SCW is under development [3]. The crucial issue of concepts is the corrosion resistance of structural materials of cladding fuel, where the most severe conditions are expected. Zirconium alloys used in current nuclear power plants cannot withstand these conditions and thus the appropriate solution is searched.

Therefore, a lot of research works [4-9] deal with the effect of SCW on corrosion behaviour and resistance of widely used structural materials. The steels with high amounts of chromium and nickel seem to be the best option from the material point of view. Iron-Nickel-chromium alloy 800 was introduced to the market in the 1950s as there was a need for heat- and corrosion-resistant alloy with relatively low nickel content. It has been widely used for its strength at high temperatures and its ability to resist oxidation, carburization, and other types of high-temperature corrosion. Alloys 800H and 800HT are austenitic with face-centred cubic crystallographic structure, solid solution alloys. Titanium nitrides, titanium carbides, and chromium carbides normally appear in the alloys' microstructure. In contrast, the austenitic stainless steel 08CH18N10T is well known steel as it is the main structural material in east nuclear power plants. This steel is instead of reducing the C content, stabilized against intergranular corrosion via alloying of Ti forming titanium carbon or titanium carbonitrides. These two materials were selected to compare and describe their corrosion behaviour during exposure to SCW. The comparison is done based on the analyses of microstructure via scanning electron microstructure involving chemical and crystallographic analyses. The oxides and oxide layers were further characterized by X-ray diffraction and Raman spectroscopy.

1. EXPERIMENTAL DETAILS

Two kinds of austenitic steels - namely 08CH18N10T (corresponds with AISI 321), 800H were exposed to SCW. The chemical composition of steels is listed in **Table 1**. The specimens for testing were cut via electric discharge machining. This was followed by grinding using sandpaper with a grit size of 30 μm.

Table 1 The chemical composition of tested materials

	Range of chemical composition (wt%)											
	C	Si	Ni	Cr	Mn	Mo	Co	Ti	Al	V	Cu	Fe
08CH18N10T	≤0.08	≤0.8	9-11	17-19	≤1.5	≤0.3	≤0.05	≥5C-0.6	-	0.2 max	0.3 max	Bal.
800H	0.05-0.10	≤1.0	30-35	19-23	≤1.5	≤0.2	≤2	0.15-0.6	0.15-0.6	-	0.75 max	Bal.

Before exposure, all specimens were ultrasonically cleaned with acetone, dried and weighed. The exposure tests were performed in the SCW loop facilities at Research Centre Řež. The exposures were carried out in demineralised water at 395 °C/25 MPa for 500 and 2700 h. The inlet/outlet conductivity of the water was measured at 2 μS/cm, while the flow rate was 5 l/h. The specimens were weighed before and after each exposure with an accuracy of 0.00001 g. After each SCW exposure period, the test coupons were air-dried immediately.

This process was followed by the examination of the oxide layer via scanning electron microscope (SEM, LYRA3 GMU) equipped with detectors for the imaging of backscatter electrons (BSE), energy dispersive spectroscopy (EDS) for chemical analysis and electron backscatter diffraction (EBSD) for crystallography analysis. For this purpose, the cross-sections of the exposed specimens were used and metallographically ground using sandpaper with a grain size of 1200, followed by polishing using a diamond paste of 3 and 1 μm. The final step consisted of using colloidal silica (OPS - oxide-polishing silica).

The oxides were also analysed via Raman spectroscopy and x-ray diffraction (XRD). For this purpose, a Nicolet DXR2 Raman microscope with an excitation laser of 532 nm was used. The power of the laser ranged from 0.1 to 10 mW and the wavelength range from 3500-50 cm^{-1} (resolution of 2 cm^{-1}). Each spectrum was composed of 100 exposures and the background was measured 50 times before the analysis. Grazing incidence X-ray diffraction (GIXRD) pattern of specimens were collected using an Empyrean 3rd generation diffractometer (Malvern-PANalytical). The diffractometer is equipped with a Co X-ray tube (X-ray wavelength 0.1789 nm, 40 kV, 40 mA), focusing X-ray mirror for Co-radiation, fixed flat-stage, and a multichannel detector PIXcel3D (1D mode). During the measurement the incident angle (ω) was fixed to 15°, while the diffraction angle 2θ varied from 15 to 125° with a step size of 0.039°. The identification of crystalline phases was performed using the High Score Plus software (PANalytical) that includes the PDF-4+ database.

2. RESULTS AND DISCUSION

As previously mentioned, the corrosion resistance of materials for further development of technologies works with SCW is crucial. Therefore, selected results based on such research are briefly introduced.

The weight changes measured after 500 hours of exposure were quite low as 0.0004 g and 0.00001g in case of 08CH18N10T and 800H, respectively. This is in accordance with the presence of crystals of oxide at the surface of both materials as can be seen in **Figure 1**. The increasing time of exposure up to 2700 h resulted in increase in dimensions and density of oxides at surfaces (see also **Figure 1**).

The oxides presented at the surfaces of both materials were analysed by SEM-EDS, Raman spectroscopy and XRD. These analyses revealed that the magnetite (Fe_3O_4, a = 8.397 Å) is formed in case of 08CH18N10T in contrast to weak peaks observed in the XRD pattern in 800H, where the most likely phase is trevorite ($NiFe_2O_4$, a = 8.347 Å).

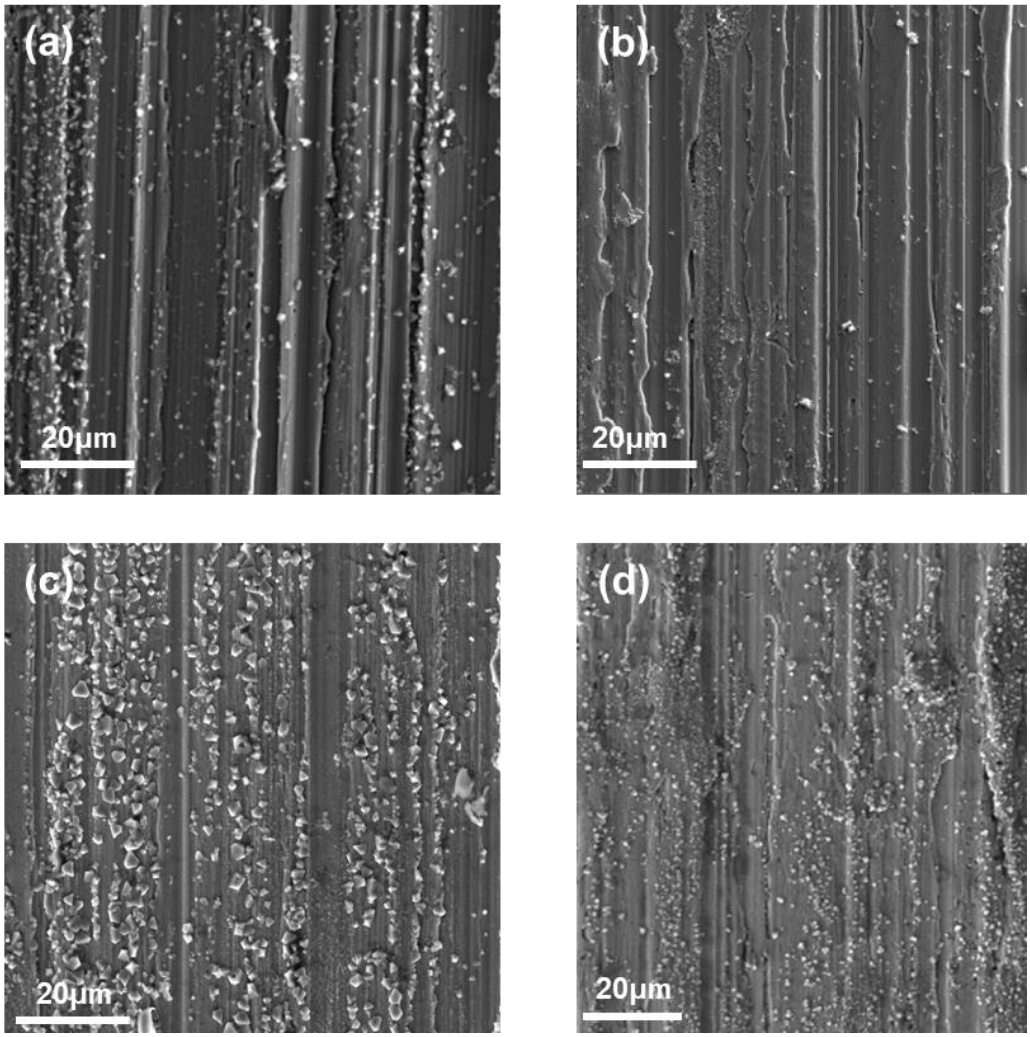

Figure 1 The surfaces of 08CH18N10T (a,c) and 800H (b,d) after exposures at 500h (a,b) and 2700h (c,d)

The very thin oxide layer can be seen in **Figure 2**, which compares the 08CH18N10T after 500h and 800H after longer exposure. as can be expected from the chemical composition being in **Table 1**. In addition, the deformation layer caused by mechanical preparation of specimens is evident in both cases.

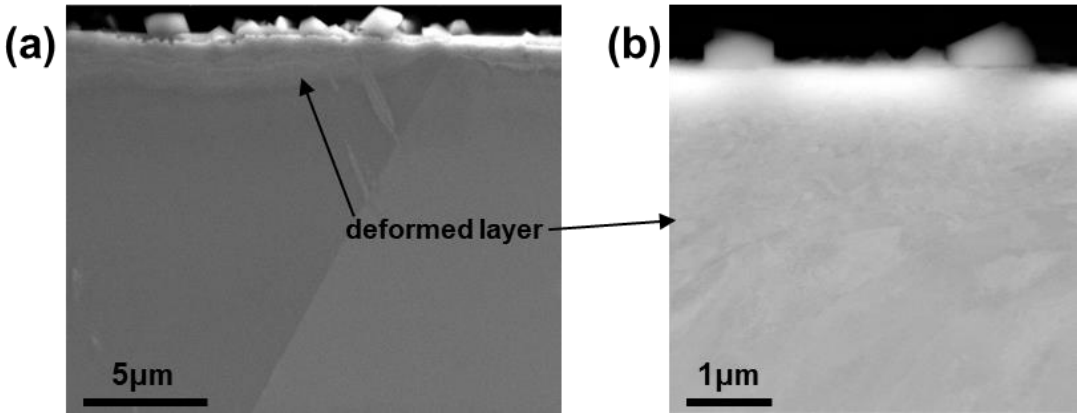

Figure 2 Cross-section of (a) 08CH18N10T (SE image) and (b) 800H (BSE image) after exposure to SCW lasted 500h and 2700h, respectively

As the layer near the surface can influence the corrosion of materials in SCW, the EBSD analysis was involved. Some results are shown in case of 800H. For this purpose, the local misorientation map was used as it can reveal residual deformation as well as a lattice distortion highlighted by green colour. The deformed layer is thus highlighted by green colour in **Figure 3** with no evidence of the fine grains as a result of the static recrystallization. The static recrystallization is usually carried out around temperature corresponding to 0.5 T_M (melting point) of the metals (T_M ~ 1400 °C), i.e. above 550 °C. It should be noted that recrystallization temperature can be decreased by alloying elements. However, near the surface the layer stay deformed also after 2700h of exposure at 395 °C in case of high alloyed 800H.

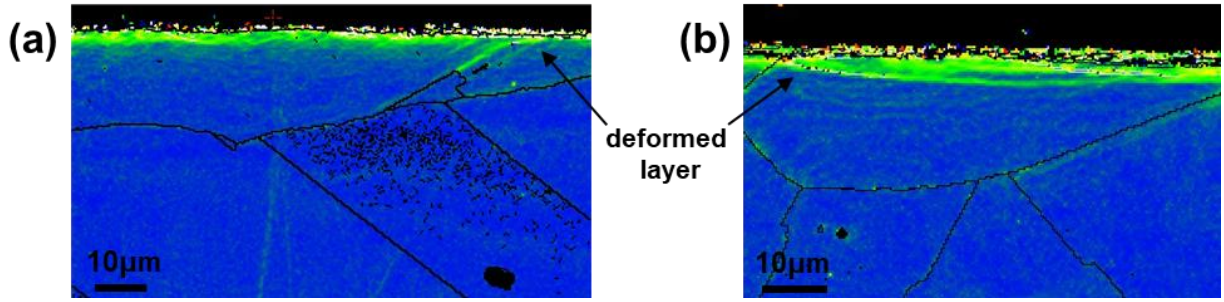

Figure 3 The local misorientation maps of 800H after exposure to SCW lasted (a) 500h and (b) 2700h.

In addition, the deformation near surface can further influence diffusion of alloying elements important for corrosion protection of materials. However, the composition of the oxide layer is also affected by the other parameters e.g. the amount of dissolved oxygen, temperature resulting in various oxides, which can be lined up according to their thermodynamic stability as follows: $NiO < MoO_2 < FeO < Fe_3O_4 < Fe_2O_3 < (Cr,Fe)_3O_4 < (Cr,Fe)_2O_3 < Cr_2O_3 < MnO < SiO_2 < Al_2O_3$ [10]. In general, the exposure of austenitic steels to SCW environments resulted in the formation of a dual oxide layer structure [4] with the outer one usually containing Fe_3O_4 and Fe_2O_3 [10,11] as was confirmed by Raman spectroscopy, XRD in case of 08CH18N10T. The alloy 800H contains a high amount of nickel and thus it can be considered the transition alloy between stainless steel and Ni-based alloys. Therefore, the composition of the oxide layer is different and as was previously mentioned, the XRD analysis identified trevorite as oxide presented on the surface. The EDS point analysis also revealed Cr and Al to be presented in that oxide. However, as the crystals of oxides are quite small these results can be subjected to error. The Raman spectroscopy was used in case of shorter exposure and the spectral bands were assigned to Fe_3O_4 magnetite, $NiFe_2O_4$ trevorit, and $FeCr_2O_4$ chromite. The oxide formed on the surface of 800H is probably the kind of spinel based on M_3O_4, where M can be Cr, Ni, Fe, and Al in different ration and combinations as in [12].

3. CONCLUSION

The paper briefly described the results from exposures of selected materials in SCW at temperature close to the critical point of water. For this purpose, mainly the SEM involving BSE and analyses such as EDS and EBSD were used. This was completed by Raman and XRD.

The results confirmed the excellent resistance of 800H as could be expected due to a high amount of Cr and Ni. However, the 08CH18N10T proved very good resistance as the oxide layer present on the surface of the specimen was very thin after long exposure to SCW at 395 °C/25 MPa. The differences were also found in the composition of oxides. However, further research is needed in this field.

ACKNOWLEDGEMENTS

Authors would like to appreciate the financial support from ECC-SMART Grant Agreement n°945234.

REFERENCES

[1] ZHENG, H., YU, T., QU, C., LI, W. and WANG, Y. Basic Characteristics and Application Progress of Supercritical Water. *IOP Conf. Ser. Earth Environ. Sci.*. 2020, no. 1, vol. 555.

[2] GUZONAS, D., NOVOTNY, R., PENTILLA, S., TOIVONEN, A. and ZHENG, W. *Materials and Water Chemistry for Supercritical Water-cooled Reactors*. 2018.

[3] SCHULENBERG, T. and OTIC, I. Suggestion for design of a small modular SCWR. *Conf. Proc. ISSCWR-10.* [Online]. 2021. Available from: https://doi.org/10.1115/1.4052191.

[4] RODRIGUEZ, D. and CHIDAMBARAM, D. Oxidation of stainless steel 316 and Nitronic 50 in supercritical and ultrasupercritical water. *Appl. Surf. Sci.* 2015, vol. 347, pp. 10-16.

[5] POUR-ALI, S., KIANI-RASHID, A. R. and BABAKHANI, A. Surface nanocrystallization and gradient microstructural evolutions in the surface layers of 321 stainless steel alloy treated via severe shot peening. *Vacuum*. 2017, vol. 144, pp. 152-159.

[6] PENTTILÄ, S., TOIVONEN, A., LI, J., ZHENG, W. and NOVOTNY, R. Effect of surface modification on the corrosion resistance of austenitic stainless steel 316L in supercritical water conditions. *J. Supercrit. Fluids*. 2013, vol. 81, pp. 157-163.

[7] TAN, L., RAKOTOJAONA, L., ALLEN, T. R., NANSTAD, R. K., and BUSBY, J. T. Microstructure optimization of austenitic Alloy 800H (Fe-21Cr-32Ni). *Mater. Sci. Eng. A*. 2011, vol. 528, no. 6, pp. 2755-2761.

[8] TAN, L., SRIDHARAN, K., and ALLEN, T. R. The effect of grain boundary engineering on the oxidation behavior of INCOLOY alloy 800H in supercritical water. *J. Nucl. Mater.* 2016, vol. 348, no. 3, pp. 263-271.

[9] TAN, L., SRIDHARAN, K., ALLEN, T. R., NANSTAD, R. K., and MCCLINTOCK, D. A. Microstructure tailoring for property improvements by grain boundary engineering. *J. Nucl. Mater.* 2008, vol. 374, no. 1-2, pp. 270-280.

[10] BEHNAMIAN, Y.*et al.* Characterization of oxide scales grown on alloy 310S stainless steel after long term exposure to supercritical water at 500 °C. *Mater. Charact.* 2016, vol. 120, no. 9, pp. 273-284.

[11] BEHNAMIAN, Y. *et al.* A comparative study on the oxidation of austenitic alloys 304 and 304-oxide dispersion strengthened steel in supercritical water at 650 °C. *J. Supercrit. Fluids*. 2017, vol. 119, pp. 245-260.

[12] TAN, L., ALLEN, T. R., and YANG, Y. Corrosion behavior of alloy 800H (Fe-21Cr-32Ni) in supercritical water. *Corros. Sci.* 2011, vol. 53, no. 2, pp. 703-711.